Modern Pathology (2021) 34:1373–1383
https://doi.org/10.1038/s41379-021-00786-x

ARTICLE

Calcified chondroid mesenchymal neoplasms with *FN1*-receptor tyrosine kinase gene fusions including *FGFR2, FGFR1, MERTK, NTRK1*, and *TEK*: a molecular and clinicopathologic analysis

Yajuan J. Liu[1] · Wenjing Wang[1] · Jeffrey Yeh[2] · Yu Wu[1] · Jose G. Mantilla[1] · Christopher D. M. Fletcher[3] · Robert W. Ricciotti[1] · Eleanor Y. Chen[1]

Received: 18 August 2020 / Revised: 10 February 2021 / Accepted: 13 February 2021 / Published online: 16 March 2021

Abstract

Translocations involving *FN1* have been described in a variety of neoplasms that share the presence of a cartilage matrix and may also contain a variable extent of calcification. Fusions of *FN1* to *FGFR1* or *FGFR2* have been reported in nine soft tissue chondromas, mostly demonstrated indirectly by FISH analysis. Delineation of *FN1* fusions with various partner genes will facilitate our understanding of the pathogenesis and diagnostic classification of these neoplasms. In this study, we present molecular, clinical, and pathologic features of 12 cartilaginous soft tissue neoplasms showing a predilection for the TMJ region and the distal extremities. We analyzed for gene fusions with precise breakpoints using targeted RNA-seq with a 115-gene panel. We detected gene fusions in ten cases, including three novel fusions, *FN1-MERTK*, *FN1-NTRK1*, and *FN1-TEK*, each in one case, recurrent *FN1-FGFR2* fusion in five cases, *FN1-FGFR1* in one case, and *FGFR1-PLAG1* in one case. The breakpoints in the 5′ partner gene *FN1* ranged from exons 11–48, retaining the domains of a signal peptide, FN1, FN2, and/or FN3, while the 3′ partner genes retained the transmembrane domain, tyrosine kinase (TK) domains, and/or Ig domain. The tumors are generally characterized by nodular/lobular growth of polygonal to stellate cells within a chondroid matrix, often accompanied by various patterns of calcification, resembling those described for the chondroblastoma-like variant of soft tissue chondroma. Additional histologic findings include extensive calcium pyrophosphate dihydrate deposition in two cases and features resembling tenosynovial giant cell tumor (TGCT). Overall, while the tumors from our series show significant morphologic overlap with chondroblastoma-like soft tissue chondroma, we describe findings that expand the morphologic spectrum of these neoplasms and therefore refer to them as "calcified chondroid mesenchymal neoplasms." These neoplasms represent a spectrum of chondroid/cartilage matrix-forming tumors harboring *FN1*-receptor TK fusions that include those classified as soft tissue chondroma as well as chondroid TGCT.

Introduction

Translocation events involving *FN1* have been described in a wide variety of neoplasms, all of which share the presence of a cartilage matrix with or without a variable extent of calcification [1–3]. Specifically, synovial chondromatosis, characterized by multinodular growth of mature cartilaginous tissue with clustering of chondrocytes has recently been shown as frequently harboring the *FN1-ACVR2* translocation [2]. The fusion of *FN1* to *FGFR1* or *FGFR2* has also been described in soft tissue chondroma, particularly in examples showing grungy to lacy (chondroblastoma-like) calcification [2]. Phosphaturic mesenchymal tumor, frequently harboring *FN1-FGFR1* or *FN1-FGF1* fusions, shows variable histologic features, and is generally characterized as a proliferation of bland spindled to stellate

Supplementary information The online version contains supplementary material available at https://doi.org/10.1038/s41379-021-00786-x.

✉ Yajuan J. Liu
yajuan@uw.edu

✉ Eleanor Y. Chen
eleanor2@uw.edu

[1] Department of Laboratory Medicine and Pathology, University of Washington, Seattle, WA, United States

[2] Department of Biology, University of Washington, Seattle, WA, United States

[3] Department of Pathology, Brigham and Women's Hospital and Harvard Medical School, Boston, MA, United States

cells with associated flocculent-appearing calcified, chondroid or ossified matrix within a highly vascularized stroma [3, 4]. Lastly, calcifying aponeurotic fibroma, a proliferation of bland fibroblastic cells with calcified fibrocartilage-like nodules, have been shown to harbor recurrent *FN1-EGF* gene fusions [1]. Besides these four entities, similar histologic features may be seen in a wide spectrum of cartilaginous neoplasms of soft tissue. These include so-called chondroid tenosynovial giant cell tumor (TGCT), calcium pyrophosphate dihydrate (CPPD) deposition disease (tophaceous pseudogout), and chondroblastoma [5–9]. These tumors in some cases share overlap in cytomorphology and histologic features, sometimes making precise histologic classification challenging.

In this study, we present the molecular, clinical, and pathologic features of 12 cases of soft tissue tumors with a chondroid matrix showing an anatomic predilection for the temporomandibular joint (TMJ) as well as the distal extremities and define a group of tumors harboring *FN1* gene fusions which we will refer to as calcified chondroid mesenchymal neoplasms. We also review the literature and discuss the relevant differential diagnosis of various entities highlighting their overlapping and distinct histologic and molecular features.

Methods and materials

Study design and case selection

Our pathology group has noted the similarity in morphologic features among tumors in our archives initially classified as various entities such as "chondroid TGCT," "tophaceous pseudogout," or simply "chondroid neoplasm", for which the differential diagnosis included chondroid TGCT, tophaceous pseudogout, and chondroma. In order to investigate whether these lesions represented distinct entities or a morphologic spectrum of related entities, 12 such cases (nine from the University of Washington Department of Pathology Archives and three from the archived cases sent in consultation to CDMF at the Brigham and Women's Hospital) were retrieved and histologic slides were independently reviewed by four pathologists (EYC, RWR, JGM, and CDMF). All cases were subjected to targeted RNA sequencing using the ArcherDX FusionPlex panel. Clinical, pathologic, and molecular findings were recorded.

This project was approved by the Institutional Review Board at the University of Washington.

Targeted RNA sequencing

All twelve specimens used in this study were archived formalin-fixed paraffin-embedded (FFPE) tissue specimens. Total nucleic acid (TNA) was extracted from the FFPE specimens using AllPrep DNA/RNA FFPE kit according to the manufacturer's recommended protocol (Qiagen, Valencia, CA, USA). The Fusionplex RNA-sequencing assay was performed using a customized 115-gene panel covering a wide spectrum of cancer genes known for their involvement in gene fusions in neoplasia including, but not limited to, *FN1*, *CSF1*, *FGFR1*, and *FGFR2* (ArcherDx, Inc. Boulder, CO). The methods for Fusionplex RNA-sequencing analysis have been described previously [10]. The genes analyzed by Fusionplex including their corresponding NM transcript identification numbers are listed in Table S1.

Sanger sequencing confirmation

For the positive fusions detected by targeted RNA-seq, RT-PCR and Sanger sequencing were performed to confirm the fusions and breakpoints at the RNA level. Once cDNAs were synthesized by random priming with Fusionplex reagent kit (ArcherDX, Boulder, CO, USA), they were subjected to a polymerase chain reaction (PCR) using FastStart Taq Polymerase (Roche Diagnostics, Indianapolis, IN, USA) with specific primers designed for each partner gene (Supplemental Materials and Methods). PCR products were cloned using TOPO TA Cloning Kit (Invitrogen, Carlsbad, CA, USA) and then were Sanger-sequenced using Eurofins Genomics Tube Sequencing service (Eurofins Genomics, Louisville, KY, USA).

Results

Clinical and pathologic findings

Our series of 12 patients includes six women and six men with a mean age of 55.7 years (range 22–72 years). Anatomic locations include the TMJ and/or temporal bone in six cases (50%), hand/digits in five cases (42%), and foot in one case (8%). Tumor size, when available, ranged from 0.5 to 4.0 cm (mean 3.1 cm). All tumors were removed by surgical excision. Follow-up information was available for three cases, with a mean duration of 1.7 years. No recurrence or metastasis was reported in any case. See Table 1 for complete clinicopathologic information.

Histologically, all tumors showed multinodular architecture and chondroid to the cartilaginous matrix (Fig. 1A, B, cases 2 and 4) with increased cellularity towards the periphery of the nodules. The matrix frequently showed calcification that was coarse or grungy to lacey (chondroblastoma-like) (Figs. 1C, D and 5A, cases 2, 4, and 11). Remarkably, the grungy calcifications in cases 5 and 12 were intensely basophilic, appeared crystalline (Case 5 shown in Fig. 2A,

Table 1 Clinicopathological features and molecular characterization of gene fusions.

Number	Original diagnosis	Age	Sex	Location	Size (cm)	Recurrence	Metastasis	Fusion (5′ exon::exon 3′)[a]	Genomic coordinates [hg19]
1	Chondroid neoplasm of synovium	70	M	TMJ[b]	4.0	NA[c]	NA	*FN1* → *FGFR2* (E15::E7)[d]	chr2:216274286,chr10:123279683
2	Atypical chondroid neoplasm	66	F	TMJ	3.9	No (1 year)	No	*FN1* → *FGFR2* (E42/ E38::E5)[e]	chr2:216232586/ chr2:216238045, chr10:123310973
3	Chondroid tenosynovial giant cell tumor	69	F	Foot	3.8	No (1 year)	No	*FN1* → *FGFR2* (E31::E5)	chr2:216246935,chr10:123310973
4	Chondroid tenosynovial giant cell tumor	52	F	Hand	0.5	NA	NA	*FN1* → *FGFR2* (E11::E5)	chr2:216285396,chr10:123310973
5	Tophaceous pseudogout	72	F	TMJ	Unknown	NA	NA	*FN1* → *FGFR2* (E17::E5)	chr2:216272831,chr10:123310973
6	Tophaceous pseudogout	44	M	TMJ	Unknown	NA	NA	*FGFR1* → *PLAG1* (E1::E3)	chr8:38325499,chr8:57083748
7	Chondroid tenosynovial giant cell tumor	36	M	Fifth finger-palm	Unknown	NA	NA	*FN1* → *FGFR1* (E25::E9)[f]	chr2:216256355,chr8:38277253
8	Chondrocalcinosis (tophaceous pseudogout)	51	M	Thumb	Unknown	NA	NA	*FN1* → *MERTK* (E24::E2)	chr2:216259251,chr2:112686697
9	Giant cell-rich lesion with chondroid stroma	49	M	Temporal/external auditory canal	Unknown	NA	NA	*FN1* → *TEK* (E27::E13)	chr2:216251412,chr9:27202818
10	Chondroid tenosynovial giant cell tumor	22	F	TMJ/temporal	3.5	No	No	No fusion detected	
11	Chondroid tenosynovial giant cell tumor	68	F	Index finger	2	NA	NA	*FN1* → *NTRK1* (E21::E7)	chr2:216263980,chr1:156841415
12	Tophaceous pseudogout	69	M	Finger	4	NA	NA	No fusion detected	

[a]Exon numbers were based on the transcript numbers of genes used for *FN1* (NM_002026.2), *FGFR2* (NM_000141.4), *MERTK* (NM_006343.2), *FGFR1* (NM_015850.3), *TEK* (NM_000459), and *PLAG1* (NM_002655.2).

[b]*TMJ* temporomandibular joint.

[c]*NA* not available.

[d]Only breakpoints reported for *FN1-FGFR2* fusion [2].

[e]Two alternatively spliced variants detected in case 2.

[f]Breakpoints differ from what was reported for the *FN1-FGFR1* fusions detected in phosphaturic mesenchymal tumors [3, 12, 27, 28].

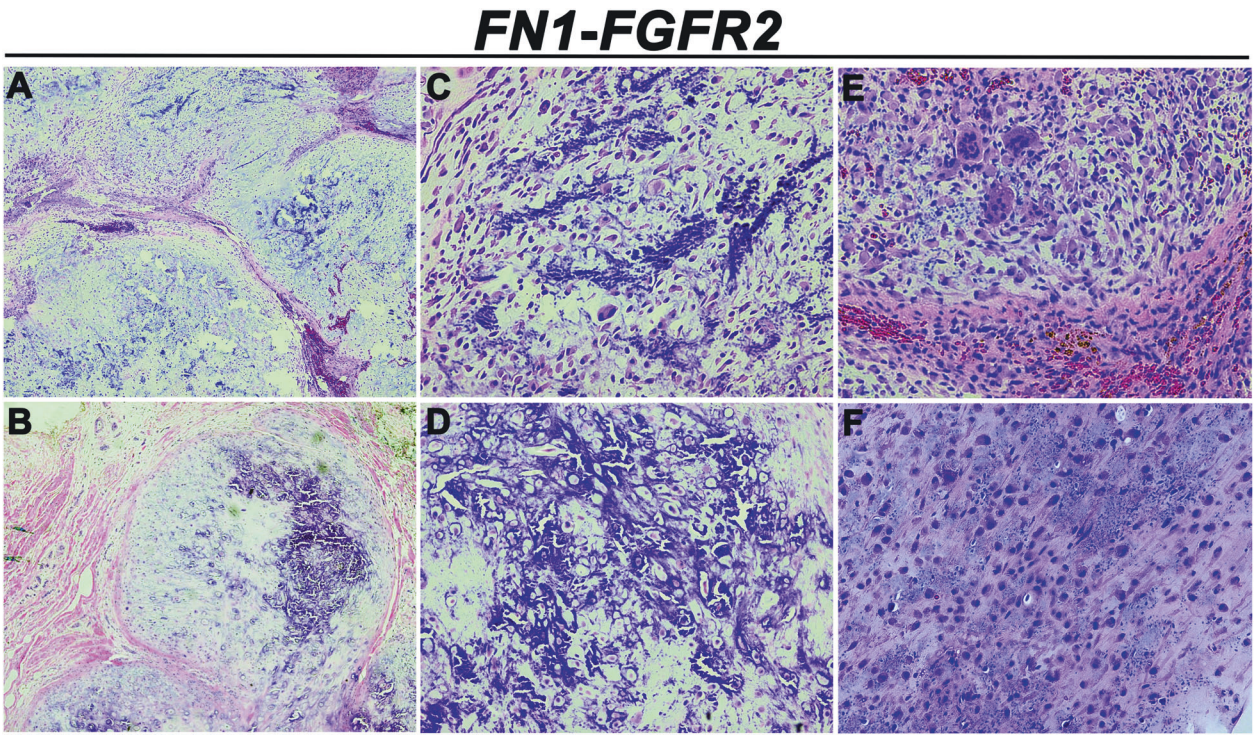

Fig. 1 Histologic features of case 2 and case 4 with *FN1-FGFR2* fusion. A, **B** Characteristic lobular architecture. **C**, **D** Grungy to lacey (chondroblastoma-like) calcifications. **E**, **F** Polygonal to spindled cells within the chondroid matrix frequently associated with osteoclast-like giant cells, while septa separating lobules contain spindled, fibroblastic cells. Panels (**A**), (**C**), and (**E**) represent case 2. Panels (**B**), (**D**), and (**F**) represent case 4.

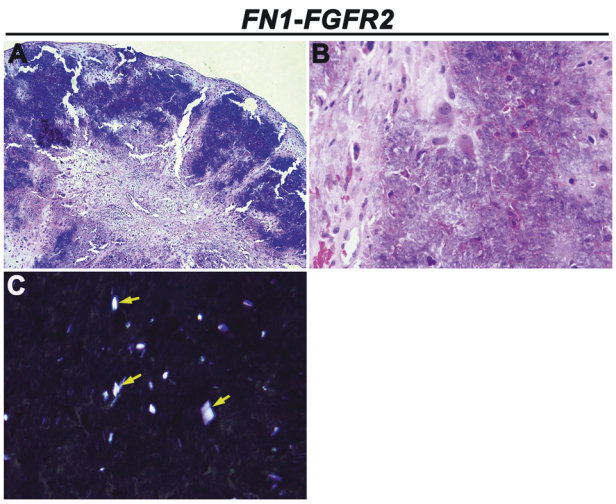

Fig. 2 Case 5 (*FN1-FGFR2* fusion) with CPPD crystal deposition. A, **B** Case 5 with extensive basophilic grungy calcification at low power (**A**) and epithelioid to differentiated chondrocytes within crystalline deposits at high power (**B**). **C** Refractile rhomboid crystals (some indicated by arrows) when viewed using polarized light consistent with CPPD.

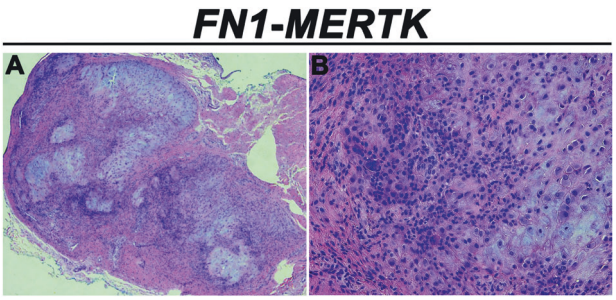

Fig. 3 Histologic features of case 7 with *FN1-MERTK* fusion. A Vaguely lobular architecture with circumscribed tumor border [2]. **B** Cells within the variably chondroid matrix and collagenous stroma are polygonal to oval with eosinophilic cytoplasm and eccentrically placed nuclei.

B), and examination using polarized light revealed refractive rhomboid crystals consistent with CPPD deposition (Fig. 2C). The tumor cells within the chondroid/cartilage matrix were polygonal to stellate with abundant eosinophilic cytoplasm and eccentrically placed nuclei with small nucleoli, while the cells in fibrous septa were more often smaller and spindled with fibroblastic features (Figs. 3A–C, 4A–D, and 5A, B, cases 2, 3, 8–11). Osteoclast-like giant cells were present in all cases and careful examination could often find at least focal areas resembling TGCT (epithelioid to histiocytoid cells with eccentric nuclei and occasionally hemosiderin deposition) in most cases (Fig. 4A–D). TGCT-like features were particularly prominent in cases 9 and 10 (Fig. 4A–D), which also had the least amount of chondroid stroma.

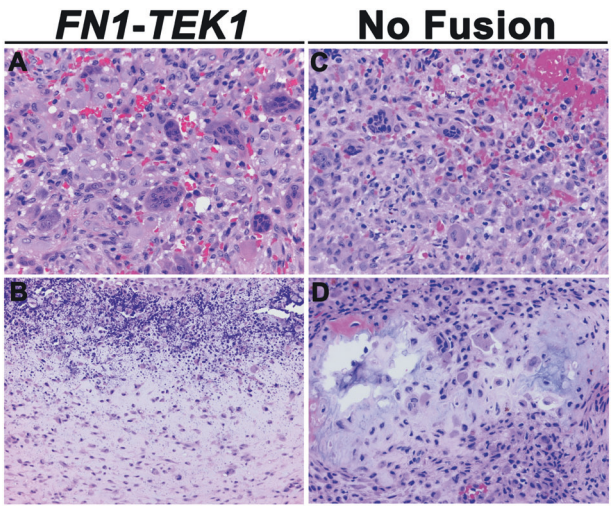

Fig. 4 Calcified chondroid mesenchymal neoplasm in this study with features resembling tenosynovial giant cell tumor (TGCT). **A**, **B** Case 9 predominantly shows the histologic features of epithelioid cells with eccentric nuclei admixed with osteoclast-like giant cells, resembling some features of TGCT (**A**) as well as a focal area of epithelioid to stellate cells in a chondroid matrix with calcification (**B**). **C**, **D** Case 10 occurring in the TMJ for comparison with case 9 showing mononuclear epithelioid/histiocytoid cells with eccentric nuclei and ring-like distribution of cytoplasmic hemosiderin as well as multinucleated giant cells (**C**). The focal area of chondroid metaplasia is present (**D**).

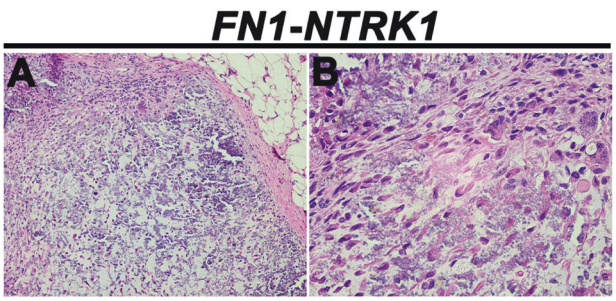

Fig. 5 Histologic features of case 11 with *FN1-NTRK1* fusion. **A** Lobular growth pattern with chondroid matrix and grungy calcifications. **B** Ovoid to spindled cells with eccentric nuclei and eosinophilic cytoplasm within the chondroid matrix. Occasional osteoclast-like giant cells are seen.

Molecular findings

An in-frame gene fusion was detected in 10 of the 12 tumors tested. The fusion genes of 10 tumors were comprised of *FN1* as the 5′ partner gene and various 3′ partner genes including *FGFR2* in 5 cases (cases 1–5), *FGFR1* in one case (case 7), and novel partner genes *MERTK*, *TEK*, and *NTRK1* in three cases (cases 8, 9 and 11, respectively) (Table 1, Fig. 6). An *FGFR1-PLAG1* fusion gene was detected in 1 tumor with *FGFR1* as the 5′ partner and *PLAG1* as the 3′ partner (case 6). All fusion transcripts were further verified by RT-PCR and Sanger sequencing (Fig. S1). No gene fusion was detected in case 10 and case 12.

Gene fusions involved various breakpoints within the coding sequence of the 5′ partner gene *FN1*, ranging from the 3′ end of exon 11 to exon 48, retaining the signal peptide domain (SP), all FN type 1 domains (FN1 binding assembly domain), and FN type 2 domains, and up to sixteen FN type 3 domains (Fig. 6). The various 3′ partner genes of the fusion transcripts had breakpoints at the 5′ ends of exon 5 to exon 7 of *FRGR2* in 5 cases, exon 9 of *FGFR1*, exon 2 of *MERTK*, exon 7 of *NTRK1*, and exon 13 of *TEK* (Fig. 6, Table 1), retaining transmembrane domain (TM) and tyrosine kinase (TK) domain in all eight cases. However, up to two extracellular FGF-binding (Ig-like) domains were retained in the fusions, including two of three Ig-like domains (Ig2 and Ig3) of *FGFR2* in cases 2–5, Ig3 only of *FGFR2* in case 1, Ig1 and Ig2 of *MERTK* in case 8, no Ig-like domain of *FGFR1* in case 7, and no Ig-like domain of *TEK* in case 9, and no Ig-like domain of *NTRK1* in case 11 (Fig. 6, Table 1). Of note, two alternatively spliced in-frame fusion transcripts of *FN1-FGFR2* were detected in case 2, and three alternatively spliced fusion transcripts of *FN1-NTRK1* were detected in case 11 with one in-frame fusion (3′ exon 21 of *FN1* to 5′ exon 7 of *NTRK1*) and apparently two shorter out-of-frame fusions (3′ exon 21 of *FN1* to 5′ exon 8 or 10 of *NTRK1*). One tumor harbored an *FGFR1-PLAG1* fusion gene with breakpoints between exons 1 and 2 of *FGFR1* and between exons 2 and 3 of *PLAG1*.

Production of FGF23 in phosphaturic mesenchymal tumors, a subset of which harbors the *FN1-FGFR1* fusion, has been demonstrated in cases with or without osteomalacia [11]. To assess whether *FGF23* is expressed in the neoplasms of our case series, we performed RT-PCR on the eight tumor samples with sufficient RNA (cases 1–4, 7, 9, and 11) using primers against regions spanning exons 1 and 2 as well as exons 2 and 3 of *FGF23*. None of the tumor samples tested expressed *FGF23* (Fig. S2).

Discussion

In this study, we identified the presence of *FN1* fusion with genes encoding receptor TKs in ten calcified chondroid mesenchymal neoplasms as well as *FGFR1-PLAG1* in one tumor (Table 1). Gene fusions involving *FN1-FGFR2* or *FN1-FGFR1* have been recently described in a subset of soft tissue chondromas, which were mostly demonstrated indirectly using break-apart FISH probes for *FN1, FGFR1*, and/or *FGFR2* [2]. To our knowledge, only one case of soft tissue chondroma with *FN1-FGFR2* has been characterized by RNA sequencing and showed a fusion between exons 1–19 of *FN1* and exons 7–17 of *FGFR2* [2]. The breakpoints in *FN1* and *FGFR2* reported, in this case, are in the

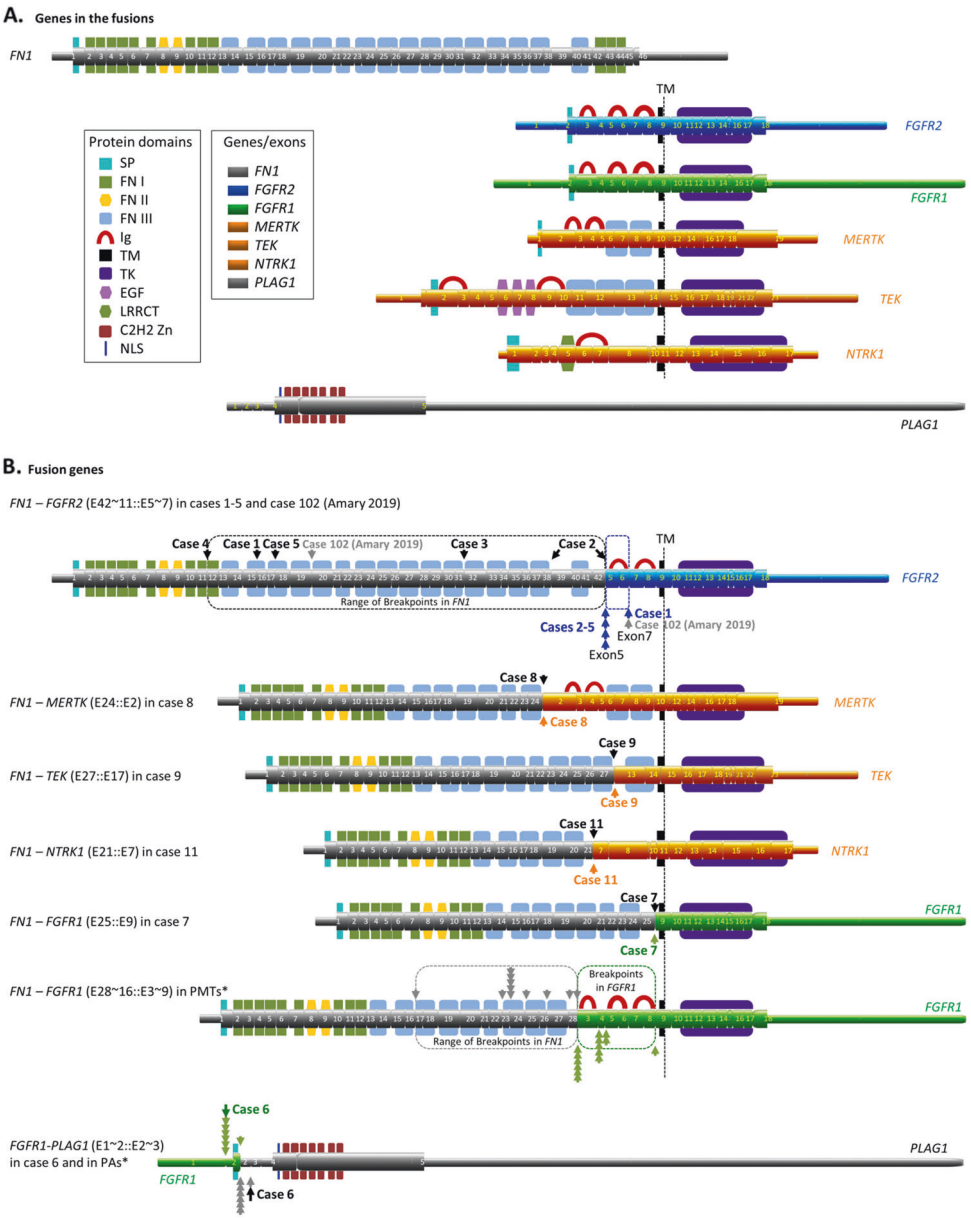

Fig. 6 Schematic of chimeric transcripts and proteins resulting from gene fusions. A RNA transcripts with exon structures and related protein domains in the genes involved in the fusions. **B** Chimeric transcripts and proteins detected in the cohort of soft tissue chondroma of this study and related tumors in the literature, showing the retained exons and functional domains of the fusion genes of *FN1, FGFR2, FGFR1, MERTK, NTRK1, TEK*, and *PLAG1*. Case 102 is the only case with *FN1-FGFR2* characterized by RNA-seq previously [2]. *PMTs = phosphaturic mesenchymal tumors with *FN1-FGFR1* fusions and range of breakpoints reported in the literature [3, 13, 26, 28, 29]. *PAs = pleomorphic adenoma of salivary gland origin with FGFR1-PLAG1 fusions and range of breakpoints reported in the literature [41]. Untranslated regions (5′ UTR and 3′ UTR) are shown as narrow bars. Exons are shown as boxes with numbers. Protein domains are represented by shapes with keys shown in the box: SP = signal peptide, FN I = FN type 1 domain, FN II = FN type 2 domain, FN III = FN type 3 domain, Ig = immunoglobulin-Like loop domain, TM = transmembrane domain, and TK = tyrosine kinase, EGF = EGF-like domain, LRRCT = leucine-rich repeat C-terminal domain, C_2H_2 Zn = C_2H_2 Zn finger, and NLS = nuclear localization signal.

range of breakpoints defined in the five tumors harboring *FN1-FGFR2* fusions in our series (Fig. 6B). We also described three novel gene fusions, *FN1-MERTK*, *FN1-TEK*, and *FN1-NTRK1* (Table 1, Fig. 6). *FN1* encodes fibronectin-1, a glycoprotein present in a dimeric form in plasma and in dimeric/multimeric forms at the cell surface and in the extracellular matrix, which participates in cell adhesion and migration processes [12]. All fusion partners of *FN1* detected in our series encode for receptor TKs; these include FGFR2 (fibroblast growth factor receptor 2),

FGFR1, MERTK (MER proto-oncogene, TK), TEK (TEK TK, endothelial), NTRK1 (neurotrophic receptor TK). These fusions result in the in-frame fusion of the N-terminal region of FN1 to the intact transmembrane and TK domains of the receptor TK, and as a result, may promote dimerization of the fused receptor through the fibronectin domain and thereby lead to aberrant signal activation as previously hypothesized [3]. The presence of fusions involving these potentially targetable receptor TKs suggests potential alternative therapeutic avenues for treating such tumors if needed.

Fusions of *FN1* to other receptor TKs have also been detected in a variety of neoplasms other than soft tissue chondroma, including *FN1-FGFR1* and *FN1–FGF1* in phosphaturic mesenchymal tumor [3, 13], *FN1-EGF* in lipofibromatosis, and calcifying aponeurotic fibroma [1, 14], *FN1-AVCR2A* in synovial chondromatosis [2], *FN1-ALK* in gastrointestinal leiomyoma and inflammatory myofibroblastic tumor [15–17], *FN1-IGF1R* in ALK-negative inflammatory myofibroblastic tumor [18], and *FN1-ROS1* in infantile inflammatory myofibroblastic tumors [19].

Soft tissue chondromas in general are characterized by nodular/lobular growth of well-differentiated chondrocytes. However, the chondroblastoma-like variant of soft tissue chondroma as described by Cates et al. also shows cellular foci of epithelioid chondrocytes of varying size admixed with osteoclast-like giant cells within a variable amount of chondroid matrix that is frequently accompanied by lace-like calcification [20]. While most cases of soft tissue chondroma have been documented to occur in the extremities, lesions involving the parotid region and skull base have been reported [21]. The cases in our series, particularly the ones with *FN1-FGFR1*, *FN1-FGFR2, FN1-NTRK1*, and *FN1-MERTK* fusions, show significant morphologic overlap with previous morphologic descriptions of the chondroblastoma-like variant of soft tissue chondroma; however, we also describe TGCT-like features as well as CPPD crystal deposition, highlighting a broader morphologic spectrum in this group of entities. We also report a larger proportion of these lesions affecting the TMJ region. We, therefore, believe that this group of neoplasms may not be best classified as simply a variant of soft tissue chondroma and have chosen to apply the term "calcified chondroid mesenchymal neoplasm" for the purposes of this study.

A few of the cases in our series warrant special consideration (see a summary of differential diagnosis in Table 2). Two tumors (case 5 in the TMJ and case 12 in the finger) showed extensive deposition of calcium pyrophosphate dehydrate (CPPD) crystals. The *FN1-FGFR2* fusion was identified in case 5. Tophaceous pseudogout is a mass-forming (tumoral) deposition of CPPD crystals that has been described in a number of locations near joints including the TMJ and some show erosion into the skull base [7, 22, 23]. Cellular infiltrates resembling foreign body type giant cell reaction are typically present, and cartilage/chondroid tissue (supposedly metaplastic) may also be seen in a significant subset of examples [7, 23]. Cates et al. previously observed CPPD deposition in one of their chondroblastoma-like soft tissue chondromas [19]. Given that one fusion-positive case in our series also contained CPPD deposition, these observations call into question whether tumoral (massive) tophaceous pseudogout, or at least a subset of cases with chondroid stroma, may actually represent neoplasms harboring recurrent gene fusions including *FN1*.

For the one tumor in our series harboring an *FN1-FGFR1* fusion gene (Fig. 6B, case 7), we considered the possibility of phosphaturic mesenchymal tumor (PMT). PMTs can take on a wide range of histologic appearances, but in general are characterized as having a highly vascular stroma (some with hemangiopericytoma-like pattern) with bland spindled to stellate neoplastic cells and amorphous basophilic chondro-osseous matrix with grungy calcification [4, 24, 25]. A significant subset of PMT was also shown to harbor *FN1-FGFR1* fusions and are frequently associated with hypophosphatemia and tumor-induced osteomalacia secondary to the paraneoplastic secretion of fibroblast growth factor 23 (FGF23) [3, 13]. Examples of PMT without apparent tumor-induced osteomalacia, however, have also been described [25] as well as fusion-negative cases that frequently overexpress α-klotho, a transmembrane enzyme that acts as an FGF23 activator [26]. α-Klotho interacts directly with FGFR1 and forms a high-affinity binding site at the Ig3 domain for FGF23 [27]. None of the cases in our series, including the one with *FN1-FGFR1*, exhibited the highly vascular stroma or spindle cell proliferation typical of PMT and none of these patients had any known osteomalacia. Furthermore, unlike most *FN1-FGFR1* fusions characterized by sequencing in PMT which retained mostly all 3 or 2 of Ig domains of *FGFR1* [3, 13, 28, 29], the *FN1-FGFR1* fusion in case 7 did not contain any Ig domains of *FGFR1* (Fig. 6B). Without the Ig3 domain, the *FN1-FGFR1* fusion protein could not interact with FGF23. By RT-PCR, we also did not detect the expression of *FGF23* in the eight tumor samples with either *FN1-FGFR1* fusion, *FN1-FGFR2*, *FN1-TEK*, or *FN1-NTRK1* (Fig. S2). Given these findings, we believe case 7 in our series does not represent PMT and is best classified as a calcified chondroid mesenchymal neoplasm. A recent description of *FN1-FGFR1* fusions in three cases of soft tissue chondroma was indirectly demonstrated using break-apart FISH probes for *FN1* and *FGFR1* without the knowledge of protein domains retained [2]. It would be informative to assess whether these three cases retain any Ig

Table 2 Summary of the differential diagnosis for calcified chondroid mesenchymal neoplasm (CCMN) (current study).

Characteristics	CCMN (current study)	Soft tissue chondroma	Chondroblastoma	Phosphaturic mesenchymal tumor	Chondroid TGCT	CPPD Tophus	Synovial chondromatosis
Median/average age	50 s	40–50 s	20 s	50 s	40–60 s	60 s	40 s
Site	Extremities and TMJ	Extremities	Long, flat, and short bones	Extremities (95%), head and neck (5%)	TMJ (most common), other sites: ear, groin	TMJ, hip, vertebrae, toe	Knee (most common) extremities, hip
Margins	Well-circumscribed	Well-circumscribed	Well-circumscribed	Well-circumscribed or infiltrative	Well-circumscribed	Well-circumscribed	Well-circumscribed
Growth pattern/ appearance	Lobular/nodular	Lobular/nodular	Lobular or sheet-like	Variegated	Lobular/nodular	Lobular	Lobular/nodular
Matrix	Chondroid with or without calcifications	Chondroid, the chondroblastoma-like variant with lace-like pericellular calcifications	chondroid, some with calcifications of various patterns (including classic lace-like)	Grungy calcifications, chondroid/osteoid matrix, rich capillary network, woven bone production	Chondromyxoid, hyaline cartilage metaplasia or chondro-osseous with frequently lace-like, pericellular grungy calcifications	Grungy calcifications, occasional chondroid metaplasia	Mature cartilage with frequent enchondroossification and/or calcifications
Cytomorphology	Polygonal to spindled mononuclear cells	Mature chondrocytes, a chondroblastoma-like variant with polygonal, stellate to spindled chondrocytes	Uniform round to polygonal mononuclear cells with well-defined border and nuclear grooves	Bland spindle cells (except for malignant form)	Proliferation of large epithelioid and small histiocytoid monocular cells admixed with histiocytes (some hemosiderin-laden) and lymphocytes	Needle to rhomboid-shaped crystals, associated with histiocytes and occasionally osteoclast-like giant cells	Mature round to polygonal chondrocytes
Osteoclast-like giant cells	Yes	Yes	Yes	Yes	Yes	Yes	No
Other features	Some with CPPD deposition	Some with ossification or CPPD deposition	Secondary aneurysmal bone cyst-like changes, woven bone matrix	Intralesional fat, chondromyxoid fibroma-like, reparative giant cell granuloma-like, angiomyolipoma-like, oxalate-like crystals			Secondary chondrosarcoma arising in <10%
Molecular findings	*FN1-FGFR2, FN1-FGFR1 (without Ig-domain), FN1-MERTK, FN1-TEK1, FN1-NTRK1*	*FN1-FGFR2*, *FN1-FGFR1* (without Ig domain)	*H3F3B* mutation (K36M)	*FN1-FGFR1* with FGF23 expression; *FN1–FGF1*	*CSF1* fusion in a subset of conventional TGCTs		*FN1–ACVR2A*
Recurrence potential	Limited follow-up	Y	Y	Y	Y	N	Y
Metastasis potential	Limited follow-up	N	Y (rare, <5%)	Y (Malignant form)	N	N	Y (secondary chondrosarcoma)
Reference		[2, 19, 20]	[8, 36, 38, 39]	[4, 12, 23, 24, 27]	[5, 9, 32–34]	[7, 21, 22]	[2]

domain. The lack of significant levels of FGF23 in these three cases of soft tissue chondromas suggest a potential lack of Ig domains in their fusions. In all, our study has demonstrated the effectiveness of RNA-seq as a tool for identifying functional domains retained in gene fusions and in turn facilitating correlation of molecular findings with clinicopathological features and tumor classification.

We detected an *FGFR1-PLAG1* in one case involving the TMJ. *FGFR1-PLAG1* fusions have been previously detected in pleomorphic adenoma (PA) of salivary gland origin and, in such cases, the 5′-portion of *FGFR1*, excluding the TK domain, is fused to the entire *PLAG1* coding sequence [30, 31]. This fusion gene arrangement is the same as that found in case 6 of our series. While PA is principally defined histologically by the proliferation of ductal and myoepithelial cells within hyalinized to the myxoid stroma, cartilaginous components may also be seen and can be quite extensive [32]. Our case was entirely composed of lobular cartilaginous tissue with variable, often grungy, calcification without any identifiable ductal or myoepithelial population and therefore histologically appeared essentially indistinguishable from the other chondroblastoma-like soft tissue chondromas in our series. In such an archived case, excluding the possibility of a PA with extensive cartilaginous components in which ductal/myoepithelial components were either not present or not sampled is problematic; however, we found no morphologic features to classify it as PA. We must also consider the possibility that *FGFR1-PLAG1* may represent an alternate fusion gene found in non-PA soft tissue cartilaginous neoplasms.

Chondroid TGCT (or TGCT with chondroid metaplasia) is a rare tumor with a predilection for the TMJ region and skull base that often demonstrates locally aggressive growth including bone destruction [5, 6, 33–35]. Histologically, chondroid TGCT shows features of conventional TGCT, such as the sheet-like proliferation of large epithelioid to histiocytoid mononuclear cells, some with hemosiderin deposition often in a ring-like deposition around the cytoplasm, and multinucleated giant cells; however, geographic or nodular areas of the chondroid matrix are also present and frequently associated with grungy, lace-like calcifications. While the majority of conventional TGCTs have been shown to harbor *CSF1* fusions [36], this genetic event has not been demonstrated in chondroid TGCT. Most cases in our series showed at least focal morphologic features resembling TGCT, although these features were particularly prominent in cases 9 and 10. The finding of *FN1-TEK* fusion in case 9 raises the possibility that lesions previously classified as chondroid TGCT may actually fall into this group of calcified chondroid mesenchymal neoplasms with *FN1* gene fusions; however, case 10, which was originally classified as chondroid TGCT, tested negative for gene fusions, including *FN1, FGFR1, FGFR2*, and *CSF1*. It remains to be determined whether other tumors described as chondroid TGCT represent a distinct tumor type or if they harbor other gene fusions that are yet to be discovered.

Additional differential diagnostic considerations include chondroblastoma and synovial chondromatosis. Chondroblastoma most often occurs in the epiphyses of long bones but may also affect the craniofacial skeleton. Histologically, it is characterized by sheets of uniform round to polygonal mononuclear cells with distinct cell borders and grooved nuclei with scattered islands of cartilaginous differentiation often showing lacey ("chicken-wire") calcification [37]. While some of our cases show a lacey calcification pattern within the cartilaginous elements, our tumors generally lack the sheet-like cellularity and characteristic cytomorphology of chondroblastoma. Lacey (chondroblastoma-like) calcifications have also been previously described in chondroblastoma-like soft tissue chondroma [20, 21, 38]. In addition, *H3F3B* K36M mutation has been detected in greater than 90% of chondroblastomas, and immunohistochemical staining using a mutation-specific antibody has been shown to be highly sensitive and specific [39, 40]. Immunohistochemical staining for the K36M mutant was negative in one case with *FN1-FGFR2* fusion (Case 2; data not shown). Synovial chondromatosis is characterized by a strikingly nodular proliferation of fairly uniform, mature, hyaline, cartilaginous tissue, often with distinct clustering of chondrocytes, which involves the joint synovium, tendon sheath, or bursa. A subset of cases harbors *FN1-ACVR2A* fusion and this finding has been described as a distinguishing feature of synovial chondromatosis from soft tissue chondroma [2]. While the tumors in our series do show lobulated growth of cartilaginous tissue, they lack the distinct clustering of chondrocytes and are negative for the *FN1-ACVR2* fusion gene. Overall, our findings indicate that the tumors in our series represent distinct entities from both chondroblastoma and synovial chondromatosis.

In summary, of the 12 tumors we analyzed, we described ten examples harboring gene fusions. In nine tumors, we detected *FN1* fusions with receptor TK genes including *FN1-FGFR2* and *FN1-FGFR1*, as well as the novel fusions *FN1-MERTK*, *FN1-TEK*, and *FN1-NTRK1*. Unlike the *FN1-FGFR1* fusions found in PMT, the *FN1-FGFR1* fusion detected in our series did not retain the Ig3 domain of the FGF23 binding site. While the cases in our series showed morphologic overlap with chondroblastoma-like soft tissue chondroma, we also reported the rare finding of extensive CPPD crystal deposition in one fusion-positive case as well as TGCT-like features, which were extensive in two cases (one fusion-positive). We, therefore, are expanding the morphologic spectrum of tumors with *FN1*-receptor TK fusions beyond those previously described as soft tissue chondroma and therefore propose the term calcified

chondroid mesenchymal neoplasm. Our findings also raise the question of whether some lesions previously classified as tophaceous pseudogout (particularly with chondroid stroma) and chondroid TGCT may actually represent neoplasms within this spectrum harboring recurrent *FN1* gene fusions. The presence of *FGFR1-PLAG1* in one of our cases suggests that PA of salivary gland origin should be considered in the differential diagnosis of cartilage forming lesions affecting the craniofacial region. While most of these tumors are amenable to surgical excision, the structure of these fusion genes indicates that therapeutic targeting of the receptor TKs may be a promising alternative treatment avenue if needed.

Data availability

The datasets generated and/or analyzed during the current study are available from the corresponding author on reasonable request.

Acknowledgements

Funding This project was supported by intra-departmental funds. No external funding was used for the study.

Author contributions YJL, EYC, and RWR performed study concept and design; YJL, WW, and YW performed methodology development, technical support, and validation; YJL, WW, JY, YW, JGM, CDMF, RWR, and EYC performed data acquisition, analysis, or interpretation; YJL, RWR, and EYC wrote the manuscript; YJL, RWR, EYC, CDMF, and JGM revised the manuscript. All authors read the approved the final manuscript.

Compliance with ethical standards

Ethics approval/consent to participate This retrospective study was approved by the Institutional Review Board at the University of Washington (protocol #9362). No human subjects were recruited for the study. The study has been performed in accordance with the Declaration of Helsinki.

Conflict of interest The authors declare no competing of interests.

Publisher's note Springer Nature remains neutral with regard to jurisdictional claims in published maps and institutional affiliations.

References

1. Puls F, Hofvander J, Magnusson L, Nilsson J, Haywood E, Sumathi VP, et al. FN1-EGF gene fusions are recurrent in calcifying aponeurotic fibroma. J Pathol. 2016;238:502–7.
2. Amary F, Perez-Casanova L, Ye H, Cottone L, Strobl A-C, Cool P, et al. Synovial chondromatosis and soft tissue chondroma: extraosseous cartilaginous tumor defined by FN1 gene rearrangement. Mod Pathol. 2019;32:1762–71.
3. Lee J-C, Jeng Y-M, Su S-Y, Wu C-T, Tsai K-S, Lee C-H, et al. Identification of a novel FN1-FGFR1 genetic fusion as a frequent event in phosphaturic mesenchymal tumour. J Pathol. 2015;235:539–45.
4. Folpe AL, Fanburg-Smith JC, Billings SD, Bisceglia M, Bertoni F, Cho JY, et al. Most osteomalacia-associated mesenchymal tumors are a single histopathologic entity: an analysis of 32 cases and a comprehensive review of the literature. Am J Surg Pathol. 2004;28:1–30.
5. Hoch BL, Garcia RA, Smalberger GJ. Chondroid tenosynovial giant cell tumor: a clinicopathological and immunohistochemical analysis of 5 new cases. Int J Surg Pathol. 2011;19:180–7.
6. Oda Y, Izumi T, Harimaya K, Segawa Y, Ishihara S, Komune S, et al. Pigmented villonodular synovitis with chondroid metaplasia, resembling chondroblastoma of the bone: a report of three cases. Mod Pathol. 2007;20:545–51.
7. Ishida T, Dorfman HD, Bullough PG. Tophaceous pseudogout (tumoral calcium pyrophosphate dihydrate crystal deposition disease). Hum Pathol. 1995;26:587–93.
8. Konishi E, Nakashima Y, Mano M, Tomita Y, Kubo T, Araki N, et al. Chondroblastoma of extra-craniofacial bones: clinicopathological analyses of 103 cases. Pathol Int. 2017;67:495–502.
9. Wang J-G, Liu J, He B, Gao L, Zhang L, Liu J. Diffuse tenosynovial giant cell tumor around the temporomandibular joint: an entity with special radiologic and pathologic features. J Oral Maxillofac Surg. 2019;77:1022.e1–1022.e39.
10. Tretiakova MS, Wang W, Wu Y, Tykodi SS, True L, Liu YJ. Gene fusion analysis in renal cell carcinoma by FusionPlex RNA-sequencing and correlations of molecular findings with clinicopathological features. Genes Chromosomes Cancer. 2020;59:40–9.
11. Bahrami A, Weiss SW, Montgomery E, Horvai AE, Jin L, Inwards CY, et al. RT-PCR analysis for FGF23 using paraffin sections in the diagnosis of phosphaturic mesenchymal tumors with and without known tumor induced osteomalacia. Am J Surg Pathol. 2009;33:1348–54.
12. Zollinger AJ, Smith ML. Fibronectin, the extracellular glue. Matrix Biol. 2017;60–61:27–37.
13. Lee J-C, Su S-Y, Changou CA, Yang R-S, Tsai K-S, Collins MT, et al. Characterization of FN1-FGFR1 and novel FN1-FGF1 fusion genes in a large series of phosphaturic mesenchymal tumors. Mod Pathol. 2016;29:1335–46.
14. Al-Ibraheemi A, Folpe AL, Perez-Atayde AR, Perry K, Hofvander J, Arbajian E, et al. Aberrant receptor tyrosine kinase signaling in lipofibromatosis: a clinicopathological and molecular genetic study of 20 cases. Mod Pathol. 2019;32:423–34.
15. Haimes JD, Stewart CJR, Kudlow BA, Culver BP, Meng B, Koay E, et al. Uterine inflammatory myofibroblastic tumors frequently harbor ALK fusions with IGFBP5 and THBS1. Am J Surg Pathol. 2017;41:773–80.
16. Panagopoulos I, Gorunova L, Lund-Iversen M, Lobmaier I, Bjerkehagen B, Heim S. Recurrent fusion of the genes FN1 and ALK in gastrointestinal leiomyomas. Mod Pathol. 2016;29:1415–23.
17. Ouchi K, Miyachi M, Tsuma Y, Tsuchiya K, Iehara T, Konishi E, et al. FN1: a novel fusion partner of ALK in an inflammatory myofibroblastic tumor. Pediatr Blood Cancer. 2015;62:909–11.
18. Piarulli G, Puls F, Wängberg B, Fagman H, Hansson M, Nilsson J, et al. Gene fusion involving the insulin-like growth factor 1 receptor in an ALK-negative inflammatory myofibroblastic tumour. Histopathology. 2019;74:1098–102.
19. Lopez-Nunez O, John I, Panasiti RN, Ranganathan S, Santoro L, Grélaud D, et al. Infantile inflammatory myofibroblastic tumors: clinicopathological and molecular characterization of 12 cases. Mod Pathol. 2020;33:576–90.
20. Cates JM, Rosenberg AE, O'Connell JX, Nielsen GP. Chondroblastoma-like chondroma of soft tissue: an

underrecognized variant and its differential diagnosis. Am J Surg Pathol. 2001;25:661–6.
21. Raparia K, Lin JW, Donovan D, Vrabec JT, Zhai QJ, Ayala AA, et al. Chondroblastoma-like chondroma of soft tissue: report of the first case in the base of skull. Ann Diagn Pathol. 2013;17:298–301.
22. Houghton D, Munir N, Triantafyllou A, Begley A. Tophaceous pseudogout of the temporomandibular joint with erosion into the middle cranial fossa. Int J Oral Maxillofac Surg. 2020;49:1286–9.
23. Kurihara K, Mizuseki K, Saiki T, Wakisaka H, Maruyama S, Sonobe J. Tophaceous pseudogout of the temporomandibular joint: report of a case. Pathol Int. 1997;47:578–80.
24. Agaimy A, Michal M, Chiosea S, Petersson F, Hadravsky L, Kristiansen G, et al. Phosphaturic mesenchymal tumors: clinicopathologic, immunohistochemical and molecular analysis of 22 cases expanding their morphologic and immunophenotypic spectrum. Am J Surg Pathol. 2017;41:1371–80.
25. Sent-Doux KN, Mackinnon C, Lee J-C, Folpe AL, Habeeb O. Phosphaturic mesenchymal tumor without osteomalacia: additional confirmation of the "nonphosphaturic" variant, with emphasis on the roles of FGF23 chromogenic in situ hybridization and FN1-FGFR1 fluorescence in situ hybridization. Hum Pathol. 2018;80:94–8.
26. Lee C-H, Su S-Y, Sittampalam K, Chen PC-H, Petersson F, Kao Y-C, et al. Frequent overexpression of klotho in fusion-negative phosphaturic mesenchymal tumors with tumorigenic implications. Mod Pathol. 2020;33:858–70.
27. Chen G, Liu Y, Goetz R, Fu L, Jayaraman S, Hu M-C, et al. α-Klotho is a non-enzymatic molecular scaffold for FGF23 hormone signalling. Nature. 2018;25:461–6.
28. Yamada Y, Kinoshita I, Kenichi K, Yamamoto H, Iwasaki T, Otsuka H, et al. Histopathological and genetic review of phosphaturic mesenchymal tumours, mixed connective tissue variant. Histopathology. 2018;72:460–71.
29. Saba KH, Cornmark L, Rissler M, Fioretos T, Åström K, Haglund F, et al. Genetic profiling of a chondroblastoma-like osteosarcoma/malignant phosphaturic mesenchymal tumor of bone reveals a homozygous deletion of CDKN2A, intragenic deletion of DMD, and a targetable FN1-FGFR1 gene fusion. Genes Chromosomes Cancer. 2019;58:731–6.
30. Katabi N, Xu B, Jungbluth AA, Zhang L, Shao SY, Lane J, et al. PLAG1 immunohistochemistry is a sensitive marker for pleomorphic adenoma: a comparative study with PLAG1 genetic abnormalities. Histopathology. 2018;72:285–93.
31. Persson F, Winnes M, Andrén Y, Wedell B, Dahlenfors R, Asp J, et al. High-resolution array CGH analysis of salivary gland tumors reveals fusion and amplification of the FGFR1 and PLAG1 genes in ring chromosomes. Oncogene. 2008;27:3072–80.
32. Klijanienko J, Servois V, Jammet P, Validire P, Pouillart P, Vielh P, et al. Pleomorphic adenoma. Am J Surg Pathol. 1998;22:772–3.
33. Fisher M, Biddinger P, Folpe AL, McKinnon B. Chondroid tenosynovial giant cell tumor of the temporal bone. Otol Neurotol. 2013;34:e49–50.
34. Carlson ML, Osetinsky LM, Alon EE, Inwards CY, Lane JI, Moore EJ. Tenosynovial giant cell tumors of the temporomandibular joint and lateral skull base: review of 11 cases. Laryngoscope. 2017;127:2340–6.
35. Anbinder AL, Geraldo BMC, Guimarães R, Pereira DL, Almeida OP, de, Carvalho YR. Chondroid tenosynovial giant cell tumor of the temporomandibular joint: a rare case report. Braz Dent J. 2017;28:647–52.
36. West RB, Rubin BP, Miller MA, Subramanian S, Kaygusuz G, Montgomery K, et al. A landscape effect in tenosynovial giant-cell tumor from activation of CSF1 expression by a translocation in a minority of tumor cells. Proc Natl Acad Sci USA. 2006;103:690–5.
37. Chen W, DiFrancesco LM. Chondroblastoma: an update. Arch Pathol Lab Med. 2017;141:867–71.
38. Kuprys TK, Bindra R, Borys D, Nystrom LM. Chondroblastoma-like chondroma of the hand: case report. J Hand Surg Am. 2014;39:933–6.
39. Behjati S, Tarpey PS, Presneau N, Scheipl S, Pillay N, Van Loo P, et al. Distinct H3F3A and H3F3B driver mutations define chondroblastoma and giant cell tumor of bone. Nat Genet. 2013;45:1479–82.
40. Amary MF, Berisha F, Mozela R, Gibbons R, Guttridge A, O'Donnell P, et al. The H3F3 K36M mutant antibody is a sensitive and specific marker for the diagnosis of chondroblastoma. Histopathology. 2016;69:121–7.
41. Dalin MG, Katabi N, Persson M, Lee K-W, Makarov V, Desrichard A, et al. Multi-dimensional genomic analysis of myoepithelial carcinoma identifies prevalent oncogenic gene fusions. Nat Commun. 2017;30:1197.